

DNS of turbulent boundary layer with time-periodic blowing through a spanwise slot

K. Kim¹ and H.J. Sung²

1. Department of Mechanical Engineering, Korea Advanced Institute of Science and Technology,
373-1, Guseong-dong, Yusong-gu, Daejeon, 305-701, Korea,

e-mail: kyoungyoun@webmail.kaist.ac.kr

2. Department of Mechanical Engineering, Korea Advanced Institute of Science and Technology,
373-1, Guseong-dong, Yusong-gu, Daejeon, 305-701, Korea,

e-mail: hjsung@kaist.ac.kr

Corresponding author H.J. Sung

Abstract

Direct numerical simulations are extended to see the effects of time-periodic blowing frequency from a spanwise slot on a turbulent boundary layer. The time-periodic blowing frequency is given in a range $0 \leq f^+ \leq 0.08$ at a fixed blowing amplitude of $A^+ = 0.5$. The effects of the blowing frequency are scrutinized by examining the phase- or time-averaged turbulent statistics. A most effective blowing frequency is obtained at $f^+ = 0.03$, where the maximum increases of Reynolds shear stress, streamwise vorticity fluctuations and energy redistribution are made. The phase-averaged stretching and tilting terms are studied for analyzing the increase of streamwise vorticity fluctuations which is closely related to turbulent coherent structures.

Keyword: *periodic blowing, spanwise slot, turbulent boundary layer, DNS, energy redistribution*

1. Introduction

Advances in the understanding the coherent structure of wall-bounded turbulent flow have intensified interest in controlling the near-wall turbulence. Recent direct numerical simulations have demonstrated a successful active control over the entire wall [1,2]. From a practical point of view, however, this active control over the entire wall is difficult to implement because it requires a dense population of sensors and actuators on the wall. Many attempts have been made to devise a practical method for controlling wall bounded flows. These include the modification of the wall surface by installing riblets [3], as well as the use of a compliant wall [4], a wall deformation [5] or a spanwise oscillating wall [6]. Among the approaches considered to date, the use of local suction/blowing [7,8] deserves more detailed study because it provides an efficient and simple means for locally actuating the wall-bounded flow. Moreover, the strength of the actuation can be controlled with relative ease by local suction/blowing.

Most previous experimental and numerical studies of local suction/blowing have focused on steady actuation [9,10,11,12]. It is reported that the local steady blowing lifts up near-wall streamwise vortices, thereby reducing the interaction of the vortices with the wall. The steady blowing leads to a reduction in the skin friction near the wall, combined with an increase in the turbulent intensity and skin friction far downstream from the slot. In contrast to the previous studies that considered only steady blowing, a relatively few studies of unsteady suction/blowing were made experimentally and numerically [13,14,15,16,17]. Park *et al.* [13] performed experiments to probe the effects of periodic blowing and suction through a spanwise slot on a turbulent boundary layer. The higher forcing frequency induces greater changes in the turbulent structures of boundary layer. Rhee and Sung [14] performed unsteady Reynolds-Averaged-Navier-Stokes simulations and compared the simulation results with those of the experiments of Park *et al.* [13]. It is known that the near-wall streamwise vortices play a dominant role on the wall-bounded flows [18], however, the responses of near-wall vortices to the unsteady periodic blowing were not studied in detail.

Report Documentation Page

Form Approved
OMB No. 0704-0188

Public reporting burden for the collection of information is estimated to average 1 hour per response, including the time for reviewing instructions, searching existing data sources, gathering and maintaining the data needed, and completing and reviewing the collection of information. Send comments regarding this burden estimate or any other aspect of this collection of information, including suggestions for reducing this burden, to Washington Headquarters Services, Directorate for Information Operations and Reports, 1215 Jefferson Davis Highway, Suite 1204, Arlington VA 22202-4302. Respondents should be aware that notwithstanding any other provision of law, no person shall be subject to a penalty for failing to comply with a collection of information if it does not display a currently valid OMB control number.

| | | | | | |
|---|------------------------------------|---|---|---------------------------------|---------------------------------|
| 1. REPORT DATE 15 APR 2005 | 2. REPORT TYPE N/A | 3. DATES COVERED - | | | |
| 4. TITLE AND SUBTITLE DNS of turbulent boundary layer with time-periodic blowing through a spanwise slot | | 5a. CONTRACT NUMBER | | | |
| | | 5b. GRANT NUMBER | | | |
| | | 5c. PROGRAM ELEMENT NUMBER | | | |
| 6. AUTHOR(S) | | 5d. PROJECT NUMBER | | | |
| | | 5e. TASK NUMBER | | | |
| | | 5f. WORK UNIT NUMBER | | | |
| 7. PERFORMING ORGANIZATION NAME(S) AND ADDRESS(ES) Department of Mechanical Engineering, Korea Advanced Institute of Science and Technology, 373-1, Guseong-dong, Yuseong-gu, Daejeon, 305-701, Korea | | 8. PERFORMING ORGANIZATION REPORT NUMBER | | | |
| | | 10. SPONSOR/MONITOR'S ACRONYM(S) | | | |
| 9. SPONSORING/MONITORING AGENCY NAME(S) AND ADDRESS(ES) | | 11. SPONSOR/MONITOR'S REPORT NUMBER(S) | | | |
| | | 12. DISTRIBUTION/AVAILABILITY STATEMENT Approved for public release, distribution unlimited | | | |
| 13. SUPPLEMENTARY NOTES See also ADM001800, Asian Computational Fluid Dynamics Conference (5th) Held in Busan, Korea on October 27-30, 2003., The original document contains color images. | | | | | |
| 14. ABSTRACT | | | | | |
| 15. SUBJECT TERMS | | | | | |
| 16. SECURITY CLASSIFICATION OF: | | | 17. LIMITATION OF ABSTRACT UU | 18. NUMBER OF PAGES 8 | 19a. NAME OF RESPONSIBLE PERSON |
| a. REPORT unclassified | b. ABSTRACT unclassified | c. THIS PAGE unclassified | | | |

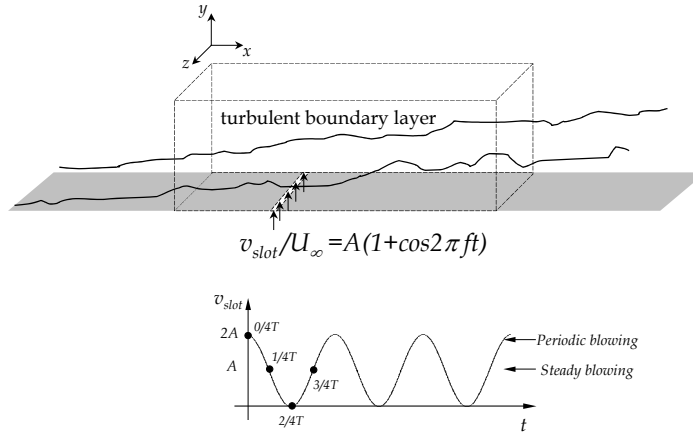


Fig. 1. Schematic diagram of the computational domain

Recently, Kim and Sung [19] performed direct numerical simulations to analyze the effects of time-periodical blowing through a spanwise slot on a turbulent boundary layer. The blowing velocity was varied in a cyclic manner from 0 to $2A^+$ ($A^+=0.25, 0.50$ and 1.00) at a fixed blowing frequency of $f^+=0.017$. The effect of steady blowing ($A^+=0$) was also examined, and the steady blowing results were compared with those of unsteady periodic blowing. The periodic blowing generates a spanwise vortical structure in the downstream of the slot. The energy redistribution is enhanced by the periodic blowing. However, it is expected that the turbulence structure is more sensitive to the blowing frequency than the blowing strength.

In the present study, the effect of the blowing frequency on turbulent boundary layer is studied as a sequel to the previous study of Kim and Sung [19]. Main emphasis of this study is placed on the blowing frequency effect on near-wall turbulent flow structures downstream of the spanwise slot. The Reynolds number based on the momentum thickness at inlet is $Re_\theta=300$, and the slot width is approximately 100 wall units. The localized time-periodic blowing is given by changing the vertical velocity on the spanwise slot. The blowing frequency is in a range of $0 \leq f^+ \leq 0.08$ at a fixed blowing amplitude ($A^+=0.5$). The frequency responses are scrutinized by examining the phase- or time-averaged turbulent statistics. A most effective blowing frequency is observed at $f^+=0.03$, where the maximum increases of Reynolds shear stress, streamwise vorticity fluctuations and energy redistribution are made.

2. Computational details

In the present study, the computational details are the same as those of the earlier work of Kim and Sung [19]. The flow configuration, boundary conditions and other numerical procedures are summarized in the following. As shown in Fig. 1, the domain size is $200\theta_{in} \times 30\theta_{in} \times 40\theta_{in}$ in the streamwise, wall-normal and spanwise directions, where the corresponding mesh size is $257 \times 65 \times 129$. The mesh is uniform in the streamwise and spanwise directions, but a hyperbolic tangent stretching is used in the normal direction to cluster points near the wall. The mesh resolutions are $\Delta x^+ \approx 12.40$, $\Delta y^+_{min} \approx 0.17$, $\Delta y^+_{max} \approx 23.86$, and $\Delta z^+ \approx 4.96$, based on the friction velocity at the inlet. Realistic velocity fluctuations at the inlet are obtained using the method of Lund *et al.* [20]. The convective outflow condition $(\partial u_i / \partial t) + c(\partial u_i / \partial x) = 0$ is used at the exit, where c is taken to be the mean exit velocity. A no-slip boundary condition is imposed at the solid wall. At the free-stream, the conditions $u=U_\infty$ and $\partial v / \partial y = \partial w / \partial y = 0$ are imposed. Periodic boundary conditions are used in the spanwise direction. The spanwise slot for periodic blowing extends from $x=75.8\theta_{in}$ to $x=82.0\theta_{in}$, where the location of the inlet is defined as $x=0$. The slot width is $b^+ \approx 100$ in wall units. The periodic blowing at the slot is generated by varying the wall-normal velocity according to the equation:

$$v_{slot} / U_\infty = A(1 + \cos 2\pi f t) \tag{1}$$

The maximum blowing velocity ($v_{slot}=2A$) is imparted at $t=0/4T$ and the minimum ($v_{slot}=0$) at $t=2/4T$, where T is the blowing period. At $t=1/4T$ and $3/4T$, the blowing velocities are the same as that of steady blowing with decelerating and accelerating phase, respectively. The amplitude of periodic blowing is $A^+=0.5$ in wall unit, which corresponds to the value of v_{rms} at $y^+=15$ without blowing. The blowing frequency ($f^+=f\nu/u_{\tau,in}^2$) varies in a range $0 \leq f^+ \leq 0.08$, where $u_{\tau,in}$ is the friction velocity at the inlet. The governing Navier-Stokes and continuity equations are integrated in time by using a fractional step method with an implicit velocity decoupling procedure [21]. A second-order central difference scheme is used in space with a staggered mesh. The Reynolds number based on the momentum thickness at the inlet is $Re_{\theta}^+=300$. The computation time step is $\Delta t U_{\infty} / \theta_{in} = 0.3$, which corresponds to $\Delta t^+ \approx 0.25$ in wall units. The total time over which statistical averages are calculated is $T_{avg} = 18000 \theta_{in} / U_{\infty}$, which corresponds to 150, 460 and 1250 periods for $f^+ = 0.01, 0.03$ and 0.08 , respectively. The imposition of periodic blowing may lead to periodic variations in the global physical quantities of the flow. Hence, it is necessary to represent each flow quantity as a superposition of three components

$$q(x, y, z, t) = \bar{q}(x, y) + \tilde{q}(x, y, t) + q''(x, y, z, t), \quad (2)$$

where the instantaneous quantity q is decomposed into a time-mean component \bar{q} , an oscillating component \tilde{q} and a random fluctuating component q'' . The time-average is

$$\bar{q}(x, y) = \frac{1}{T_{tot} L_z} \int_0^{T_{tot}} \int_0^{L_z} q(x, y, z, t) dz dt, \quad (3)$$

where $T_{tot} = NT$ is the time over which the quantity is averaged and N is the total number of periods. The oscillating component \tilde{q} is obtained from the relation

$$\tilde{q}(x, y, t) = \langle q \rangle(x, y, t) - \bar{q}(x, y) \quad (4)$$

where $\langle q \rangle(x, y, t)$ is the phase-average, which is defined as

$$\langle q \rangle(x, y) = \frac{1}{NL_z} \sum_{n=1}^N \int_0^{L_z} q(x, y, z, t) dz. \quad (5)$$

Accordingly, the random fluctuation component q'' is expressed as

$$q''(x, y, z, t) = q(x, y, z, t) - \langle q \rangle(x, y, t) \quad (6)$$

3. Results and Discussion

It is important to find the energy redistribution by the present unsteady blowing. The relative increase of turbulent intensity is defined as $\Delta\eta(\%) = (\eta_{max} - \eta_{max,o}) / \eta_{max,o} \times 100$, where the subscript "o" denotes no blowing. As displayed in Fig. 2, the increases of cross-stream components $\Delta v''_{rms}$ and $\Delta w''_{rms}$ are larger than that of streamwise component $\Delta u''_{rms}$. This means that the intercomponent energy transfer is enhanced by unsteady blowing. The behaviours of $\Delta v''_{rms}$ and $\Delta w''_{rms}$ indicate that they have a broad peak at around $f^+ = 0.03$. Next, to see the relative contribution to the turbulent kinetic energy of streamwise turbulent intensity and intensities normal to the mean flow, the energy partition parameter K^* is calculated, $K^* = 2u''^2 / (v''^2 + w''^2)$ [22]. The parameter K^* is measured at which the increase of turbulent kinetic energy is maximum. It is obvious that K^* has a local minimum at $f^+ = 0.03$. The smaller value of K^* means that the energy redistribution is more active. However, as the blowing

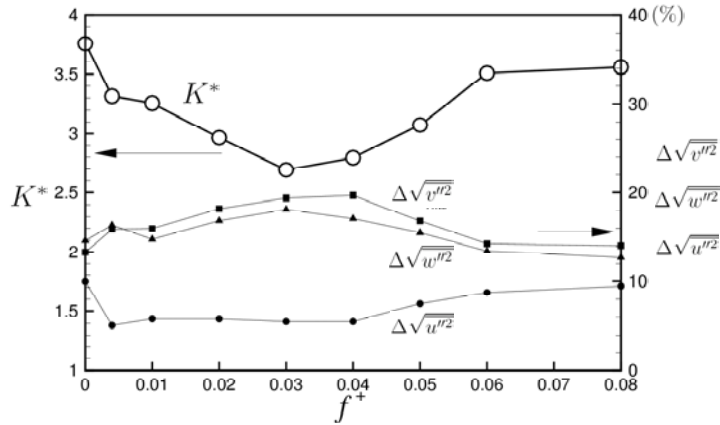


Fig. 2. Relative increases of turbulent intensities and the energy partition parameter K^*

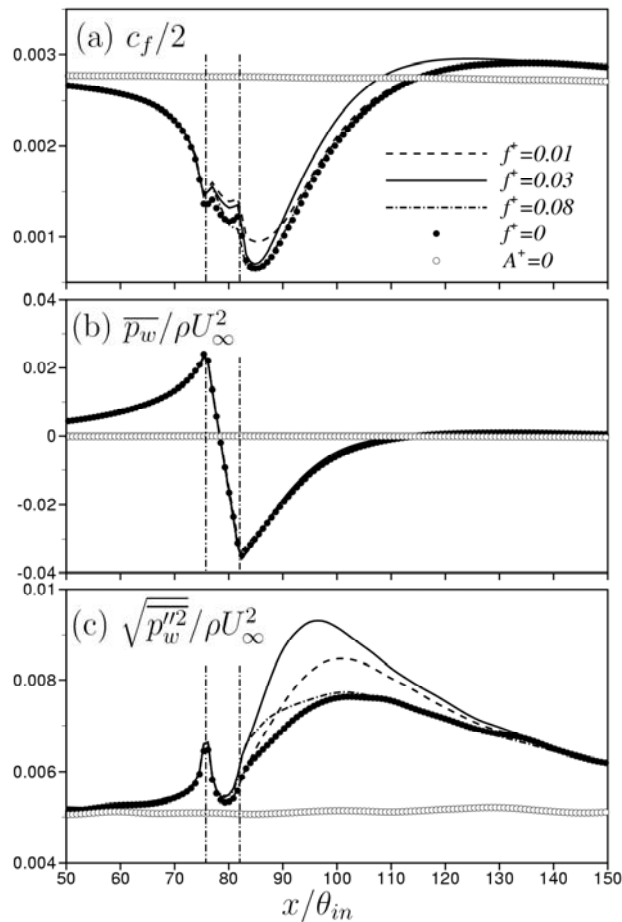


Fig. 3. Time-averaged values of (a) skin friction coefficient, (b) wall pressure, (c) wall pressure fluctuations.

frequency increases further ($f^+=0.08$), K^* converges to that of $f^+=0$. This suggests that the flow is not sensitive to the higher frequency blowing.

Figure 3 shows the streamwise distributions of time-averaged skin friction c_f , wall pressure \bar{p}_w and rms of wall pressure fluctuations $p''_{w,rms}$. Three cases of the blowing frequency ($f^+=0.01, 0.03$ and 0.08) are chosen to distinguish the flow structures by unsteady blowing. The effective blowing frequency is chosen at $f^+=0.03$, which gives the minimum value of K^* . The lower and higher blowing frequencies are chosen at $f^+=0.01$ and $f^+=0.08$, respectively. $f^+=0$ corresponds to 'steady blowing' and $A^+=0$ is 'no blowing'. For all blowing cases in Fig. 3(a), c_f decreases rapidly near the slot and increases in the downstream. It is seen that the recovery of c_f at $f^+=0.03$ is faster than other two blowing cases.

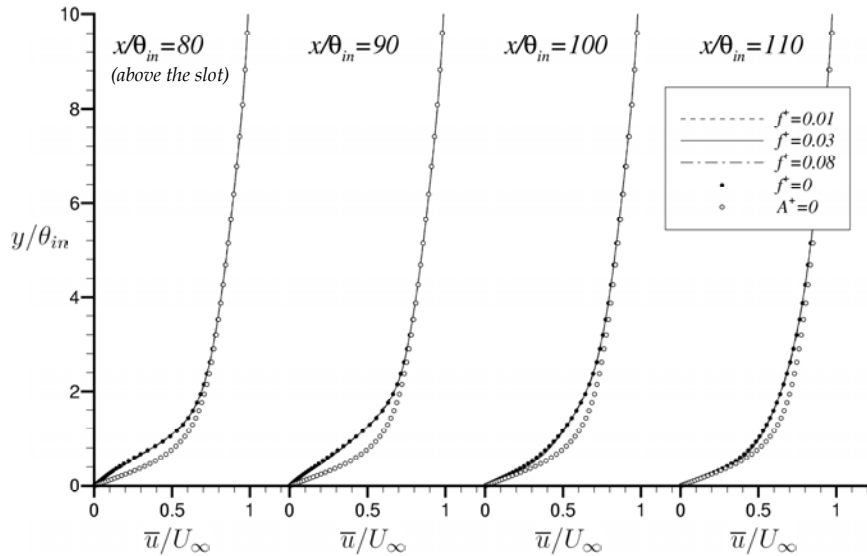


Fig. 4. Time-averaged streamwise velocity profiles

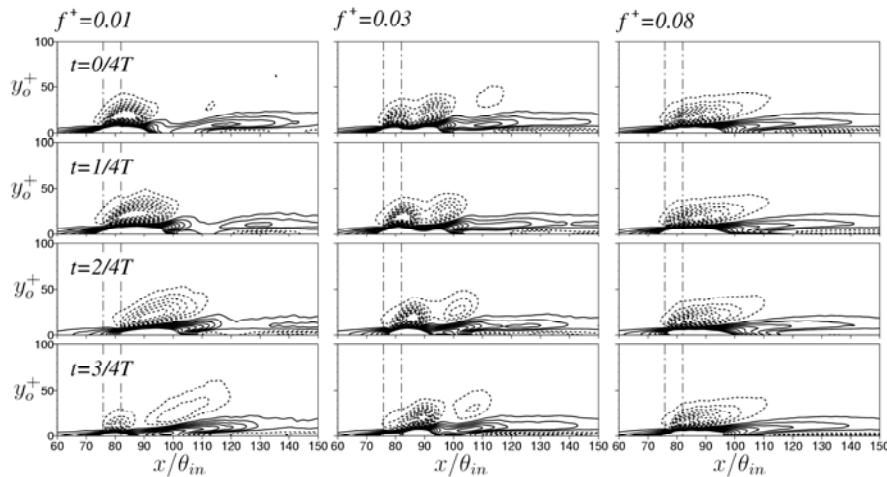


Fig. 5. Contours of $\langle \omega_z \rangle - \bar{\omega}_{z,o}$. The contour levels are from -0.25 to 0.25 by increments

However, the variations of wall pressure \bar{p}_w in Fig. 3(b) are almost the same regardless of the blowing frequency. The adverse pressure gradient appears ahead and behind the slot, whereas the favourable pressure gradient occurs above the slot. As shown in Fig. 3(c), the wall pressure fluctuations $p''_{w,rms}$ are very sensitive to the effective blowing frequency ($f^+=0.03$).

Distributions of the time-averaged streamwise velocity at four locations ($x/\theta_{in}=80, 90, 100$ and 110) are displayed in Fig. 4. As compared to the case of 'no blowing', a region of retarded flow is observed near the wall. As the flow moves downstream, the region of retarded flow gradually shifts away from the wall and finally decays. However, the time-averaged streamwise velocity is invariant with the blowing frequency. This is consistent with the previous results [16,17].

Contours of the difference between the phase-averaged spanwise vorticity for periodic blowing $\langle \omega_z \rangle$ and the time-averaged spanwise vorticity for 'no blowing' $\bar{\omega}_{z,o}$ are shown in Fig. 5 during one period ($1T$). A negative region of $\langle \omega_z \rangle - \bar{\omega}_{z,o}$, denoted by dashed line, appears above the slot for three cases. This is because a negative spanwise vorticity layer in the vicinity of the wall is shifted upward by blowing. Note that the negative (positive) value of $\langle \omega_z \rangle - \bar{\omega}_{z,o}$ represents the increase (decrease) of the magnitude of spanwise vorticity $|\omega_z|$. This is caused by the fact that $\bar{\omega}_{z,o}$ is negative inside the boundary layer. For $f^+=0.01$, it is clearly seen that a region of strong negative spanwise vorticity is formed above the slot and convects downstream as time goes by. During the accelerating phase ($t=3/4T \sim 0/4T$), the formation of the strong negative spanwise vorticity occurs above the slot, which

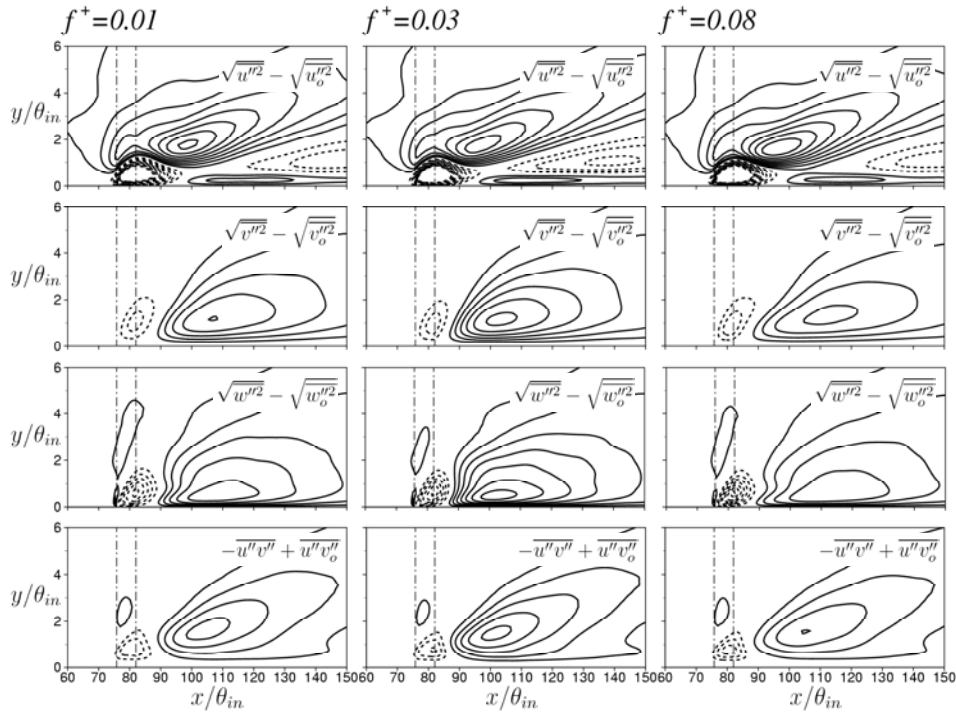


Fig. 6. Contours of the difference between the time-averaged turbulent intensities and Reynolds shear stress for periodic blowing and those for no blowing.

results from the lifted wall vorticity layer by blowing. The region of strong negative spanwise vorticity convects to downstream during the decelerating phase ($t=1/4T \sim 2/4T$), when the adverse pressure gradient decreases above the slot. For $f^+=0.03$, the lifted vorticity layer convects to lesser extent as compared with $f^+=0.01$. This may be attributed to the fact that the time difference between the accelerating and decelerating phases becomes smaller with increasing the blowing frequency. Thus, a newly generated strong spanwise vorticity coexists with the weaker prior one which convected in the decelerating phase of the previous period. For $f^+=0.08$, however, the time difference is so small that the afore-stated unsteady responses, such as the convection of the strong negative spanwise vorticity, are not found.

Figure 6 shows contours of the difference between the time-averaged rms velocity fluctuations (u''_{rms} , v''_{rms} , w''_{rms} and $-u''v''$) for blowing and the values of 'no blowing'. For three blowing cases, the turbulent intensities and Reynolds shear stress are significantly enhanced downstream of the slot. The maximum increase of u''_{rms} is located closer to the slot than those of v''_{rms} , w''_{rms} and $-u''v''$. The general contour patterns for three blowing cases look similar. However, a closer inspection of the patterns reveals that the maximum increases of v''_{rms} , w''_{rms} and $-u''v''$ for $f^+=0.03$ are located closer to the slot as compared with other blowing frequencies. This may be related to the rapid increase of c_f behind the slot for $f^+=0.03$, as mentioned earlier in Fig.3(a).

Profiles of the time-averaged rms velocity fluctuations and Reynolds shear stress are shown in Fig. 7. The velocity fluctuations and Reynolds shear stress for blowing are increased downstream of the slot compared with the case of 'no blowing'. The maximum increase of u''_{rms} is located at around $x/\theta_{in}=100$. However, the maximum increases of v''_{rms} , w''_{rms} and $-u''v''$ are located in the farther downstream ($x/\theta_{in}=110$). It is interesting to find that the increase of u''_{rms} for $f^+=0.03$ is smaller than those for other frequencies, whereas the increases of v''_{rms} , w''_{rms} and $-u''v''$ for $f^+=0.03$ are larger than those for other frequencies. This suggests that $f^+=0.03$ is the most effective blowing frequency in promoting the energy redistribution. Park *et al.* [13] reported that the transverse fluctuating components are more susceptible to disturbances than the streamwise component. On the other hand, the time-averaged turbulent intensities appear to be insensitive to the higher blowing frequency ($f^+=0.08$).

Figure 8 shows the time-averaged rms vorticity fluctuations ($\omega_i''_{rms}$). All components of the vorticity fluctuations ($\omega_x''_{rms}$, $\omega_y''_{rms}$ and $\omega_z''_{rms}$) are enhanced downstream of the slot by periodic

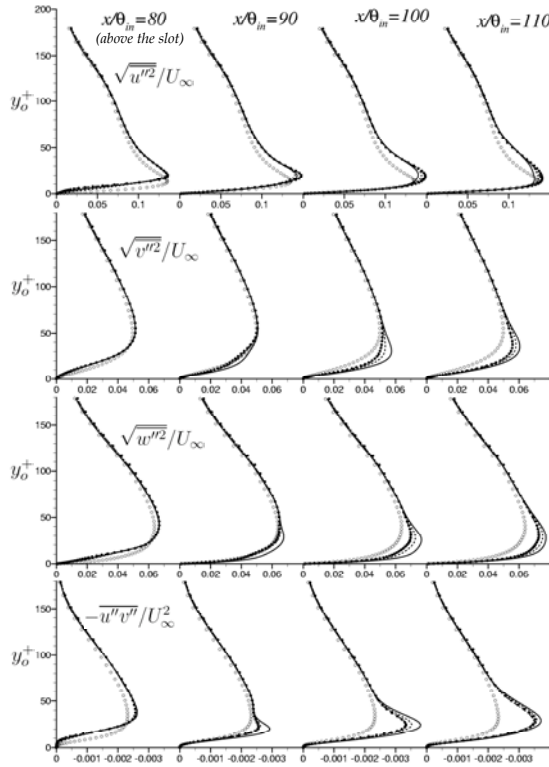


Fig. 7. Time-averaged turbulent intensities and Reynolds shear stress.

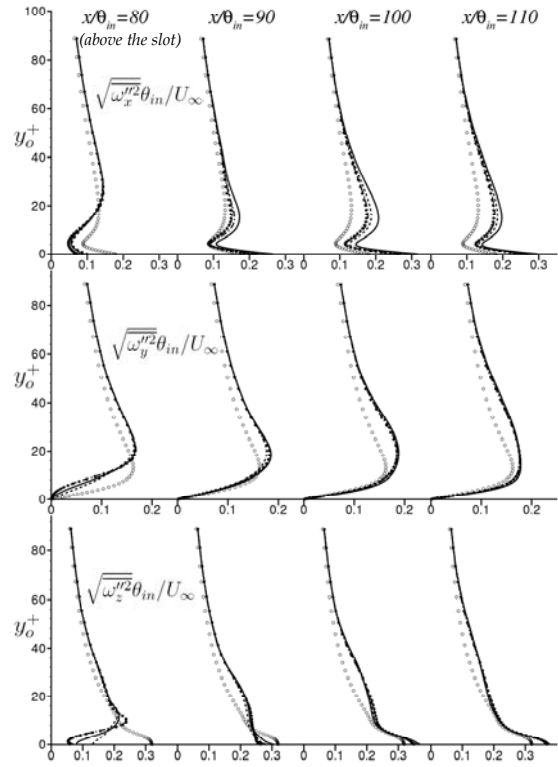


Fig. 8. Root time-mean square of vorticity fluctuations.

blowing. A closer examination of Fig. 8 indicates that $\omega_y''_{rms}$ and $\omega_z''_{rms}$ are enhanced by blowing regardless of the blowing frequency. However, $\omega_x''_{rms}$ is most enhanced at a particular blowing frequency ($f^+=0.03$). Accordingly, the most effective blowing frequency is $f^+=0.03$, at which the near-wall vortical structure is most activated. It is known that the location of local maximum of $\omega_x''_{rms}$ corresponds to that of the center of the streamwise vortex in the wall region [23]. Recall that the maximum increases of wall pressure fluctuations and Reynolds shear stress are observed at $f^+=0.03$ (Figs. 3 and 7).

Conclusion

Detailed numerical analysis has been performed to see the effect of blowing frequency on a turbulent boundary layer. The slot width is $b^+ \approx 100$ in wall units and the blowing frequency varies in a range $0 \leq f^+ \leq 0.08$ with a fixed blowing amplitude ($A^+=0.5$). An effective blowing frequency is observed at $f^+=0.03$, which gives the minimum value of K^* . The time-averaged streamwise velocity and wall pressure are invariant with the blowing frequency. However, the time-averaged skin friction and rms of wall pressure fluctuations are sensitive to the blowing frequency. Furthermore, the recovery of skin friction is fast at $f^+=0.03$. The maximum increase of u''_{rms} is located closer to the slot than those of v''_{rms} , w''_{rms} and $-u''v''$. The increase of u''_{rms} for $f^+=0.03$ is smaller than those for other frequencies, whereas the increases of v''_{rms} , w''_{rms} and $-u''v''$ for $f^+=0.03$ are larger than those for other frequencies. The time-averaged streamwise vorticity fluctuations $\omega_x''_{rms}$ is most enhanced at $f^+=0.03$, which activates the near-wall vortical structures.

Acknowledgement

This research was supported by a grant from the National Research Laboratory of the Ministry of Science and Technology, Republic of Korea.

References

- [1] Choi H., Moin P. and Kim J., "Active turbulence control for drag reduction in wall-bounded flows," *Journal of Fluid Mechanics*, Vol. 262, (1994), pp 75-110.
- [2] Hammond E.P., Bewley T. R. and Moin P., "Observed mechanisms for turbulence attenuation and enhancement in opposition-controlled wall-bounded flows," *Physics of Fluids*, Vol. 10, No. 9, (1998), pp 2421-2423.
- [3] Choi H., Moin P. and Kim J., "Direct numerical simulation of turbulent flow over riblets," *Journal of Fluid Mechanics*, Vol. 255, (1993), pp 503-539.
- [4] Choi K.S., Yang X., Clayton B.R., Glover E.J., Atlar M., Semenov B.N. and Kulik V.M., "Turbulent drag reduction using compliant surfaces," *Proceedings of the Royal Society of London Series A*, Vol. 453, (1997), pp 2229-2240.
- [5] Kim C., Jeon W.-P., Park J. and Choi H., "Effects of a localized time-periodic wall motion on a turbulent boundary layer flow," *Physics of Fluids*, Vol. 15, No. 1, (2003), pp 2142-2145.
- [6] Choi J.-I., Xu C.-X. and Sung H.J., "Drag reduction by spanwise wall oscillations in wall-bounded turbulent flows," *AIAA Journal*, Vol. 40, No. 5, (2002), pp 842-850.
- [7] Rebbeck H. and Choi K.-S., "Opposition control of near-wall turbulence with a piston-type actuator," *Physics of Fluids*, Vol. 13, No. 8, (2001), pp 265-268.
- [8] Jacobson S.A. and Reynolds W.C., "Active control of streamwise vortices and streaks in boundary layers," *Journal of Fluid Mechanics*, Vol. 360, (1998), pp 179-211.
- [9] Sano M. and Hirayama N., "Turbulent boundary layers with injection and suction through a slit. First report : Mean and turbulence characteristics," *Bull. J. Soc. Mech. Eng.*, Vol. 28, No. 239, (1985), pp 807-814.
- [10] Park J. and Choi H., "Effects of uniform blowing or suction from a spanwise slot on a turbulent boundary layer flow," *Physics of Fluids*, Vol. 11, No. 10, (1999), pp 3095-3105.
- [11] Krogstad P. Å. and Kourakine A., "Some effects of localized injection on the turbulence structure in a boundary layer," *Physics of Fluids*, Vol. 12, No. 11, (2000), pp 2990-2999.
- [12] Kim K., Sung H.J. and Chung M.K., "Assessment of local blowing and suction in a turbulent boundary layer," *AIAA Journal*, Vol. 40, No. 1, (2002), pp 175-177.
- [13] Park S.-H., Lee I. and Sung H.J., "Effect of local forcing from a spanwise slot on a turbulent boundary layer," *Experiments in Fluids*, Vol. 31, (2000), pp 384-393.
- [14] Rhee G.H. and Sung H.J., "Numerical prediction of locally-forced turbulent boundary layer," *International Journal of Heat and Fluid Flow*, Vol. 22, No. 6, (2001), pp 624-632.
- [15] Park Y.S., Park S.-H. and Sung H.J., "Influence of periodic blowing and suction on a turbulent boundary layer," *Experiments in Fluids*, (2003), in press.
- [16] Tardu S., "Near wall turbulence control by time periodical blowing," *Experimental Thermal and Fluid Science*, Vol. 16, (1998), pp 41-53.
- [17] Tardu S.F., "Active control for near-wall turbulence by local oscillating blowing," *Journal of Fluid Mechanics*, Vol. 439, (2001), pp 217-253.
- [18] Robinson S.K., "Coherent motions in the turbulent boundary layer," *Annual Review of Fluid Mechanics*, Vol. 23, (1991), pp 601-639.
- [19] Kim K. and Sung H.J., "Effects of periodic blowing from a spanwise slot on a turbulent boundary layer," *AIAA Journal*, (2003), in press.
- [20] Lund T. S., Wu X., and Squires K. D., "Generation of turbulent inflow data for spatially-developing boundary layer simulation," *Journal of Computational Physics*, Vol. 140, (1998), pp 233-258.
- [21] Kim K., Baek S. -J., and Sung H. J., "An implicit velocity decoupling procedure for the incompressible Navier-Stokes equations," *International Journal for Numerical Method in Fluids*, Vol. 38, Issue. 2, (2002), pp 125-138.
- [22] Neves J.C., Moin P., and Moser R.D., "Effects of convex transverse curvature on wall-bounded turbulence. Part 1: Time velocity and vorticity," *Journal of Fluid Mechanics*, Vol. 272, (1994), pp 349-381.
- [23] Kim J., Moin P., and Moser R., "Turbulence statistics in fully developed channel flow a low Reynolds number," *Journal of Fluid Mechanics*, Vol. 177, (1987), pp 133-166.